16th World Conference on Earthquake, 16WCEE 2017

Santiago Chile, January 9th to 13th 2017

Paper N° 1119 (Abstract ID)

Registration Code: S-Y1464686585

An attenuation relationship for deep-focus earthquakes around the Ogasawara Islands, Japan

H. Kubo[(1)], W. Suzuki[(2)], T. Kunugi[(3)], S. Aoi[(4)]

[(1)] *National Research Institute for Earth Science and Disaster Resilience, Tsukuba, Japan, hkubo@bosai.go.jp*
[(2)] *National Research Institute for Earth Science and Disaster Resilience, Tsukuba, Japan, wsuzuki@bosai.go.jp*
[(3)] *National Research Institute for Earth Science and Disaster Resilience, Tsukuba, Japan, kunugi@bosai.go.jp*
[(4)] *National Research Institute for Earth Science and Disaster Resilience, Tsukuba, Japan, aoi@bosai.go.jp*

Abstract

For an understanding of the ground-motion characteristics of deep-focus earthquakes around the Ogasawara Islands, Japan, first, we investigate the spatial distributions of strong motion indexes for past events and their attenuation relationships. The observed attenuation relationship in East Japan is lower than that in West Japan, especially at short periods, which is expected to be caused by the wave-guide effect of the subducting Pacific plate. In addition, the attenuation relationship in fore-arc of East Japan is lower at short periods than that in back-arc of East Japan because of the heterogeneous attenuation structure of upper mantle in East Japan. The attenuation relationship in the Izu Peninsula and Ogasawara Islands is not consistent with that in fore-arc of East Japan, but with that in back-arc of East Japan or West Japan. This high attenuation observed in Izu-Ogasawara region could be explained by the seismic-wave path perpendicularly propagating through the Pacific Plate. Then, we separately estimate non-geometric attenuation parameters for each deep-focus earthquake. The estimated parameters show that the intrinsic and/or scattering attenuation is weak in order of the paths to fore-arc of East Japan, back-arc of East Japan, and West Japan and Izu-Ogasawara region, and that the intrinsic and/or scattering attenuation along the path to West Japan and Izu-Ogasawara region is far stronger than those along the path to East Japan. In addition, it is suggested that the difference between short-period attenuation characteristics along the path to fore- and back-arcs of East Japan may depend on the event location probably because of the three-dimensional curved shape of the Pacific Plate. Finally, we propose an empirical equation of the attenuation relationship for the deep-focus earthquakes, which is useful to predict strong ground motions for future deep-focus earthquakes.

Keywords: Deep-focus earthquakes around the Ogasawara Islands, Japan; Ground motion attenuation relationship; Strong ground motions; Empirical equation of attenuation relationship

1. Introduction

Around the Ogasawara Islands, Japan, many deep-focus earthquakes occurred and caused strong ground motions in Japan, especially in East Japan. The 2015 deep-focus earthquake off the Ogasawara Islands (M_w 7.9), which occurred at 11:23 a.m. on May 30, 2015 (UTC), was the largest event among the deep-focus events and caused strong ground motions that were felt over whole Japan with a maximum seismic intensity of 5-upper on the Japan Meteorological Agency (JMA) scale. Thus, strong ground motions of the deep-focus events could damage a vast area of Japan and could be a non-negligible seismic risk in Japan. However, few studies have investigated their ground-motion characteristics.

In this study, to understand the ground-motion characteristics of the deep earthquakes around the Ogasawara Islands, first we investigate the spatial distributions of strong motion indexes for past events and their attenuation relationships. Then, we estimate non-geometric attenuation parameters separately for each deep-focus earthquake, and discuss non-geometric attenuation characteristics along the path to each region and the event dependence of the attenuation characteristics. Finally, we propose an empirical equation of the attenuation relationship for the deep-focus earthquakes, which can be used as a base of a ground motion prediction equation for deep-focus earthquakes.

2. Ground motion distribution and its attenuation relationship

First, we investigate spatial features of ground motions using strong-motion-index distributions. Fig. 1 shows examples of peak ground acceleration (PGA) and peak ground velocity (PGV) distributions for deep-focus earthquakes around the Ogasawara Islands, which were observed by strong-motion seismograph networks K-NET and KiK-net [1] of National Research Institute for Earth Science and Disaster Resilience (NIED) and broadband seismograph network F-net [2] of NIED. The peak value is the peak square root of the sum of squares of two orthogonal horizontal components which are low-cut filtered at 0.1 Hz. The observed strong motion indexes in East Japan are larger than those in West Japan even if they were observed at the equal epicentral distance. In addition, the ground motion amplitudes in fore-arc region of East Japan is larger than those in back-arc region of East Japan, resulting in that the observed distribution of the large ground motion area is elongated along fore-arc of East Japan. These trends are clearer in PGA than those in PGV. Ground motion amplitudes in the region between the Izu Peninsula and Ogasawara Islands seem to be equivalent to or smaller than those in Kanto region (southern part of East Japan), although Izu-Ogasawara region is closer to the epicenter. These trends are observed in both K-NET/KiK-net and F-net, which implies that these trends are not caused by the site-amplification effect because F-net stations are located on bedrock.

Then, we investigate attenuation relationship of strong ground motions. Considering the spatial features of strong ground motions in Fig. 1, we divide Japan into four regions, fore-arc region of East Japan (Group 1, blue), back arc region of East Japan (Group 2, green), West Japan (Group 3, red), and Izu-Ogasawara Region (Group 4, orange) (Fig. 2). In this grouping, we use the surface plate boundary defined by Bird [3] (dotted line in Fig. 2) and the volcanic front model in East Japan proposed by Morikawa et al. [4] (broken line in Fig. 2). Fig. 3 shows examples of attenuation relationships of PGA and PGV at K-net/KiK-net and F-net stations for each region. Fig. 4 shows examples of attenuation relationships of 5 % damped horizontal acceleration response spectra (Sa) at the periods of 0.5, 1.0, 2.0, and 4.0 s at F-net stations for each region. These figures demonstrate that the strong motion indexes in each region decrease as a function of hypocentral distance.

The comparison of the observations in East Japan (Groups 1 and 2, blue and green) and West Japan (Group 3, red) suggests that the attenuation relationship observed in East Japan is weaker than that in West Japan. For Sa, this trend is clear at short periods (<= 1 s); however, at long periods (e.g., 4 s), the difference becomes small. This result indicates that the attenuation relationship along the path from source to East Japan is weaker at short periods than that along the path to West Japan. This is expected to be caused by the presence of the subducting Pacific plate along the path to East Japan. Previous studies revealed that short-period seismic waves are efficiently guided by the Pacific plate and this results in an abnormal distribution of ground motions [e.g., 5, 6, 7]. One likely reason for the wave-guide effect is that the Pacific Plate is a high-velocity and high-Q medium compared to surroundings [e.g., 5]. Another likely reason is that the Pacific Plate has an internal quasi-

laminar structure formed by latelally elongated small-scale veloicity heterogeneities [e.g., 6, 7]. In section 3, we will construct ground motion attenuation relationships using the difference non-geometric attenuation parameters between East and West Japan.

The comparison of the observations in fore-arc of East Japan (Group 1, blue) and back-arc of East Japan (Group2, green) shows that PGA in fore-arc is smaller than that in back-arc, although this trend is not clear in PGV. For Sa, the difference between fore- and back-arcs is clear at the period of 0.5 or 1.0 s; however the difference becomes obscure at longer period. Previous studies pointed out that ground motions in fore-arc for past earthquakes were stronger than these in back-arc, and suggested that this difference is caused by the heterogeneous attenuation structure of upper mantle in East Japan [e.g., 5]. Some studies tried to introduce this regional variation of ground motion amplitudes to their empirical equations of attenuation relationships [e.g., 4, 8, 9]. For example, Dhakal et al. [8] proposed an empirical equation using two non-geometric attenuation coefficients that differ between the paths in fore- and back-arcs. In this study, we will adopt the similar approach in the proposal of empirical equation of ground motion attenuation relationships.

The difference among attenuation relationships of fore-arc of East Japan, back-arc of East Japan, and West Japan is clear in events 4, 6, and 9, although it is rather unclear in event 11. Takemura et al. [7] suggested through the waveform simulation for P waves that this event had a propagation characteristic that differs from other deep-focus earthquakes. In section 3, we will investigate the event dependence of ground motion attenuation relationship by estimating attenuation parameters separately for each event

The attenuation relationship in Izu-Ogasawara region is not consistent with that in fore-arc of East Japan, but with that in back-arc of East Japan or West Japan. This strong attenuation relationship observed in Izu-Ogasawara region can be explained as follows. The stations in Izu-Ogasawara region are mostly located above the source areas of the target deep-focus events. Hence, they would receive not the seismic waveforms guided by the subducting Pacific Plate, but the seismic waveforms perpendicularly propagating through the Pacific Plate. Saito [10] demonstrated through the waveform simulation that the seismic waveforms perpendicularly propagating through the laminar heterogeneous attenuation structure are strongly attenuated and their amplitudes largely decrease compared to those propagating along the laminar structure. In section 3, we assume that Izu-Ogasawara region and West Japan have a common attenuation characteristic.

3. Non-geometric Attenuation and empirical equation of attenuation relationship

Here, first we estimate non-geometric attenuation parameters separately for each event. Target strong motion indexes are PGA, PGV, JMA seismic intensity (INT), 5 % damped Sa. INT is calculated from three components of acceleration waveforms following JMA [11]. Sa consists of 42 periods between 0.1 and 10 s. Most studies estimating empirical equations of attenuation relationship used strong-motion data observed by strong motion networks such as K-NET and KiK-net [e.g., 9, 12]. However, there are not sufficient strong-motion data for deep-focus earthquakes because of the infrequency of the large events and ununiform distribution of ground motions. Therefore, we use F-net continuous observation data here to obtain ground motions for large and moderate earthquakes observed in whole Japan. F-net stations have two types of seismograph: broadband seismograph and strong-motion seismograph. We mainly use observed waveforms by the broadband seismograph, although we also use observations by the strong-motion seismograph in the case where the observation by the broadband seismograph was scaled out or the broadband seismograph was under maintenance. For the analysis, we use the velocity waveforms and the acceleration waveforms which were differentiated from the velocity waveforms. Table 1 is the list of 12 deep-focus events used in this study. Fig. 2 shows the used events and F-net stations. The station number in Table 1 is different among events because there are cases where one of three components could not be observed by both of the broadband and strong-motion seismograph. For the epicentral location, we refer to the unified hypocentral catalogue determined by JMA. For the depth and magnitude M, we refer to the centroid depth and moment magnitude of F-net moment tensor catalogue. To consider the observed regional variation of attenuation relationship among fore-arc of East, back-arc of East Japan, and West Japan and Izu-Ogasawara region, we use three different non-geometric attenuation coefficients in the assumed equation of attenuation relationship. Because the excitation of surface waves for deep-focus events is expected to be weak compared to that of body waves, we assume the body-wave attenuation relationship whose parameters are event-scale parameter α and hypocentral distance X:

$$\log pre = \alpha + [b_1R_1 + b_2R_2 + b_3R_3] \cdot X - \log X \quad (1)$$

where *pre* is the predicted PGA, PGV, or Sa. Note that log *pre* changes *pre*/2 in the case of INT. b_1, b_2, and b_3 are the non-geometric attenuation coefficients in fore-arc of East, back-arc of East Japan, and West Japan and Izu-Ogasawara region, respectively. R_1 is 1 and 0 at stations in fore-arc of East Japan and other regions, respectively, R_2 is 1 and 0 at stations in back-arc of East Japan and other regions, respectively, and R_3 is 1 and 0 at stations in West Japan and Izu-Ogasawara region and other regions, respectively. We estimate the intercept α and the non-geometric attenuation coefficients (b_1, b_2, b_3) for each event. In the estimation, the station-number difference among station groups is corrected and then the weight of the data in fore-arc of East Japan is doubled. The surface amplification is not considered here because F-net stations are located on bedrock.

Fig. 5 shows the estimated non-geometric coefficients (b_1, b_2, b_3) and the difference between b_1 and b_2 ($b_1 - b_2$). Although there are some variations, the trend $|b_1| < |b_2| < |b_3|$ is commonly seen. This indicates that the intrinsic and/or scattering attenuation is weak in order of the paths to fore-arc of East Japan, back-arc of East Japan, and West Japan and Izu-Ogasawara region. This trend becomes obscure in Sa at long periods. Although $|b_1|$ is not largely different from $|b_2|$, $|b_3|$ is much larger than other values. This means that the intrinsic and/or scattering attenuation along the paths to West Japan and Izu-Ogasawara region is far stronger than those along the paths to East Japan, implying that the wave-guide effect of the Pacific plate is large. These features are consistent with the observations in section 2. In addition, the closer the location of a deep-focus event is to main island of Japan (e.g., event 2 or 6), the larger the difference between b_1 and b_2 in Sa at short periods (< 1 s) is. This suggests that the difference between short-period attenuation characteristics along the path to fore- and back-arcs of East Japan may depend on the event location. This is probably because of the three-dimensional curved shape of the Pacific Plate. Fig. 6 shows the relationship between α and M for each event. The estimated values of α are related to M.

Then, we estimate an empirical equation of attenuation relationship using data of all events. We propose the body-wave attenuation relationship whose parameters are *M* and hypocentral distance *X*:

$$\log pre = a \cdot M + [b_1R_1 + b_2R_2 + b_3R_3] \cdot X - \log X + c. \quad (2)$$

To estimate the coefficients (a, b_1, b_2, b_3, c) of Eq. (2), we conduct two-step linear regression analysis [e.g., 8]. First, we estimate the intercept α for each event and the non-geometric attenuation coefficients (b_1, b_2, b_3) assuming Eq. (1) from all data. Second, we estimate the coefficients (a, c) from the estimated values of α. Fig. 7 shows the estimated coefficients of the common attenuation relationship (2) and standard deviation. The estimated non-geometric coefficients of Eq. (2) are consistent with those of Eq. (1) for each event (Fig. 5). The relationship between α and *M* from the estimated coefficients (a, c) is consistent with the estimated relationship for each event (Fig. 6).

Fig. 8 shows the comparison of F-net observations with Eq. (1) for each event and Eq. (2). Although the reproducibility of Eq. (1) is better, both Eqs. can reproduce the observations.

4. Conclusion

In this study, to understand the ground-motion characteristics of deep-focus earthquakes around the Ogasawara Islands, we investigated the spatial distributions of strong motion indexes for past events and their attenuation relationships, and estimated the non-geometric attenuation parameters for each deep-focus event. The results indicate that the non-geometric attenuation characteristics differs among the paths to three regions (fore-arc of East Japan, back-arc of East Japan, and West Japan and Izu-Ogasawara region). The complex ground motions are expected to be caused by the presence of the subducting Pacific plate and the heterogeneous attenuation structure of upper mantle in East Japan. In addition, we proposed the empirical equation of ground motion attenuation relationship for the deep-focus earthquakes. The proposed empirical equation of ground motion attenuation relationship can be used in the prediction of strong ground motions for future deep-focus earthquakes, although further studies including the estimation of site correction for deep-focus events are necessary.

5. Acknowledgements

We used the unified hypocenter catalogue determined by JMA. We also used Generic Mapping Tools [13] to draw the figures.

6. Copyrights

7. References

[1] Aoi S, Kunugi T, Nakamura H, Fujiwara H. (2011): Deployment of new strong motion seismographs of K-NET and KiK-net, in *Earthquake Data in Engineering Seismology*, Geotechnical, Geological, and Earthquake Engineering, **14**, 167–186, Springer, Dordrecht, Netherlands. doi:10.1007/978-94-007-0152-6_12.

[2] Okada Y, Kasahara K, Hori S, Obara K, Sekiguchi S, Fujiwara H, Yamamoto A. (2004): Recent progress of seismic observation networks in Japan: Hi-net, F-net, K-NET and KiK-net. *Earth Planets Space*, **56**, xv–xxviii.

[3] Bird P (2003): An updated digital model of plate boundaries. *Geochem. Geophys. Geosyst.*, **4**(3), 1027.

[4] Morikawa N, Kanno T, Narita A, Fujiwara H, Fukushima Y (2006): New additional correction terms for attenuation relations of peak amplitudes and response spectra corresponding to the anomalous seismic intensity in northeastern Japan. *Journal of Japan Association of Earthquake Engineering*, **6**, 23–40 (in Japanese with English abstract).

[5] Utsu T (1966): Regional difference in absorption of seismic waves in the upper mantle as inferred from abnormal distribution of seismic intensities. *Journal of the Faculty of Science*, **2**(4), 359–374, Hokkaido University.

[6] Furumura T, Kennett BLN (2005): Subduction zone guided waves and the heterogeneity structure of the subducted plate: Intensity anomalies in northern Japan, *J. Geophys. Res.*, **110**, B10302.

[7] Takemura S, Maeda T, Furumura T, Obara K (2016): Bonin deep-focus earthquake using seismogram envelopes of high-frequency P waveforms: Occurrence of deep-focus earthquake at the bottom of a subducting slab. *Geophys. Res. Lett.*, **43**, DOI: 10.1002/2016GL068437.

[8] Dhakal YP, Takai N, Sasatani T, (2010): Empirical analysis of path effects on prediction equations of pseudo-velocity response spectra in northern Japan, *Earthquake Engng Struct. Dyn.*, **39**, 443–461.

[9] Morikawa N, Fujiwara H (2013) A New Ground Motion Prediction Equation for Japan Applicable up to M9 Mega-Earthquake. *Journal of Disaster Research*, **8**(5), 878–888.

[10] Saito T (2006): Synthesis of scalar-wave envelopes in two-dimensional weakly anisotropic random media by using the Markov approximation. *Geophys. J. Int.*, **165**(2), 501–515.

[11] Japan Meteorological Agency (JMA) (1996): Seismic intensity. Gyosei, Tokyo (in Japanese)

[12] Si H, Midorikawa S (1999): New attenuation relationships for peak ground acceleration and velocity considering effects of fault type and site condition. *J. Struct. Constr. Eng. AIJ*, **523**, 63–70 (in Japanese with English abstract).

[13] Wessel P, Smith WHF (1998) New Improved Version of the Generic Mapping Tools Released, *Eos Transactions*, AGU, **79**, 579.

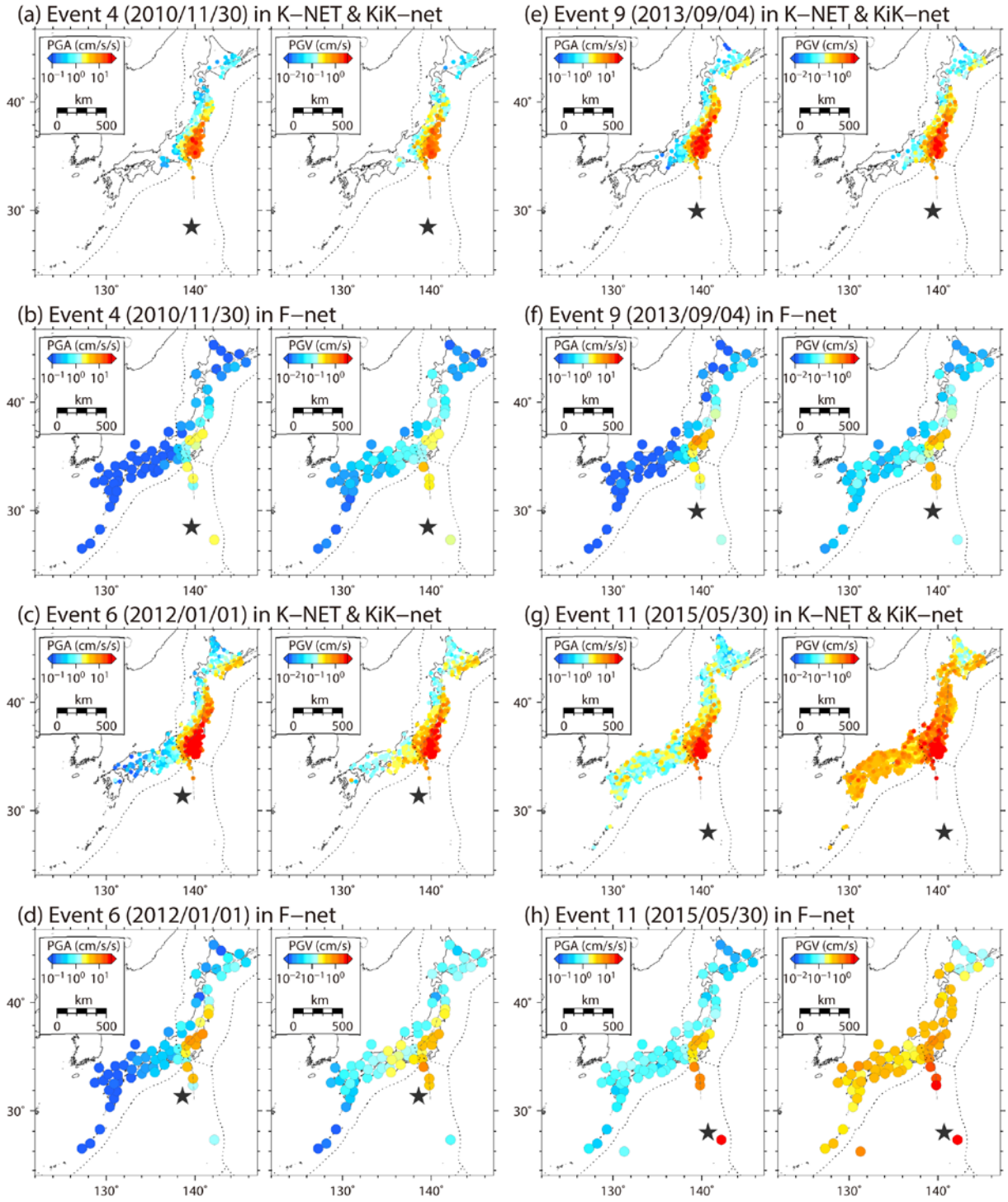

Fig. 1 – Examples of PGA and PGV distributions for deep-focus earthquakes around the Ogasawara Islands

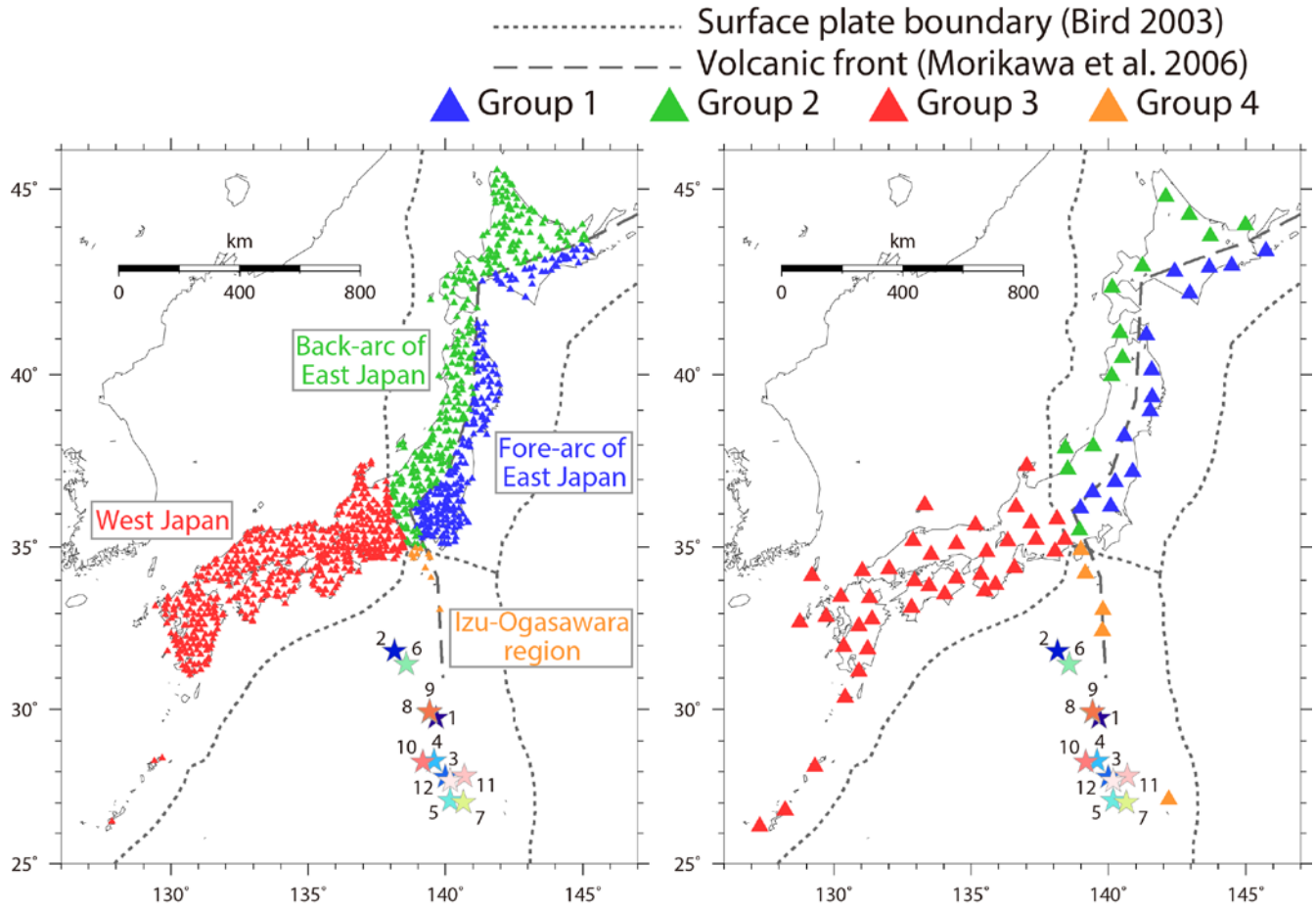

Fig. 2 – Station distributions of K-NET/KiK-net (left) and F-net (right)

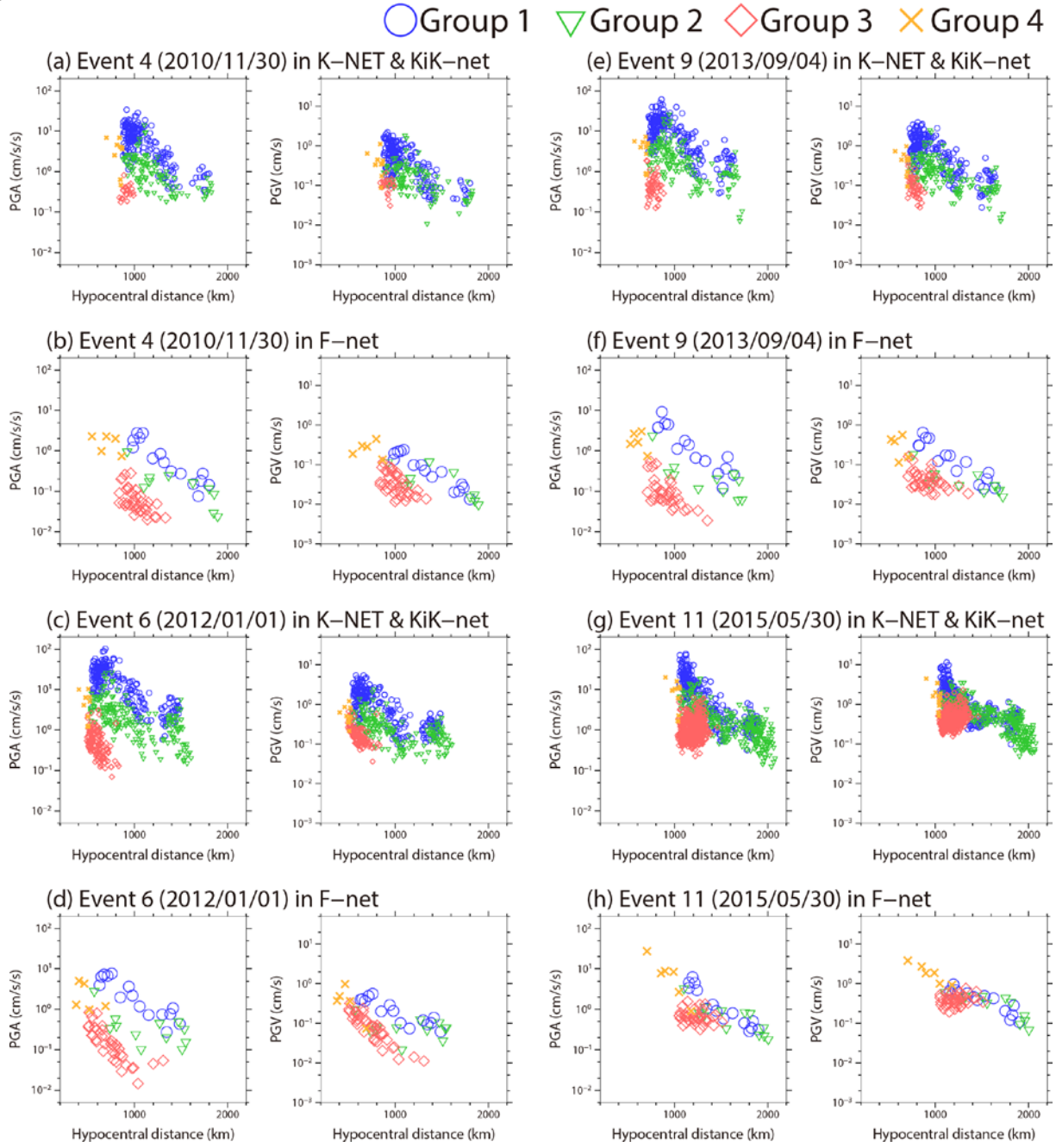

Fig. 3 – Examples of attenuation relationships of PGA and PGV for deep-focus earthquakes around the Ogasawara Islands.

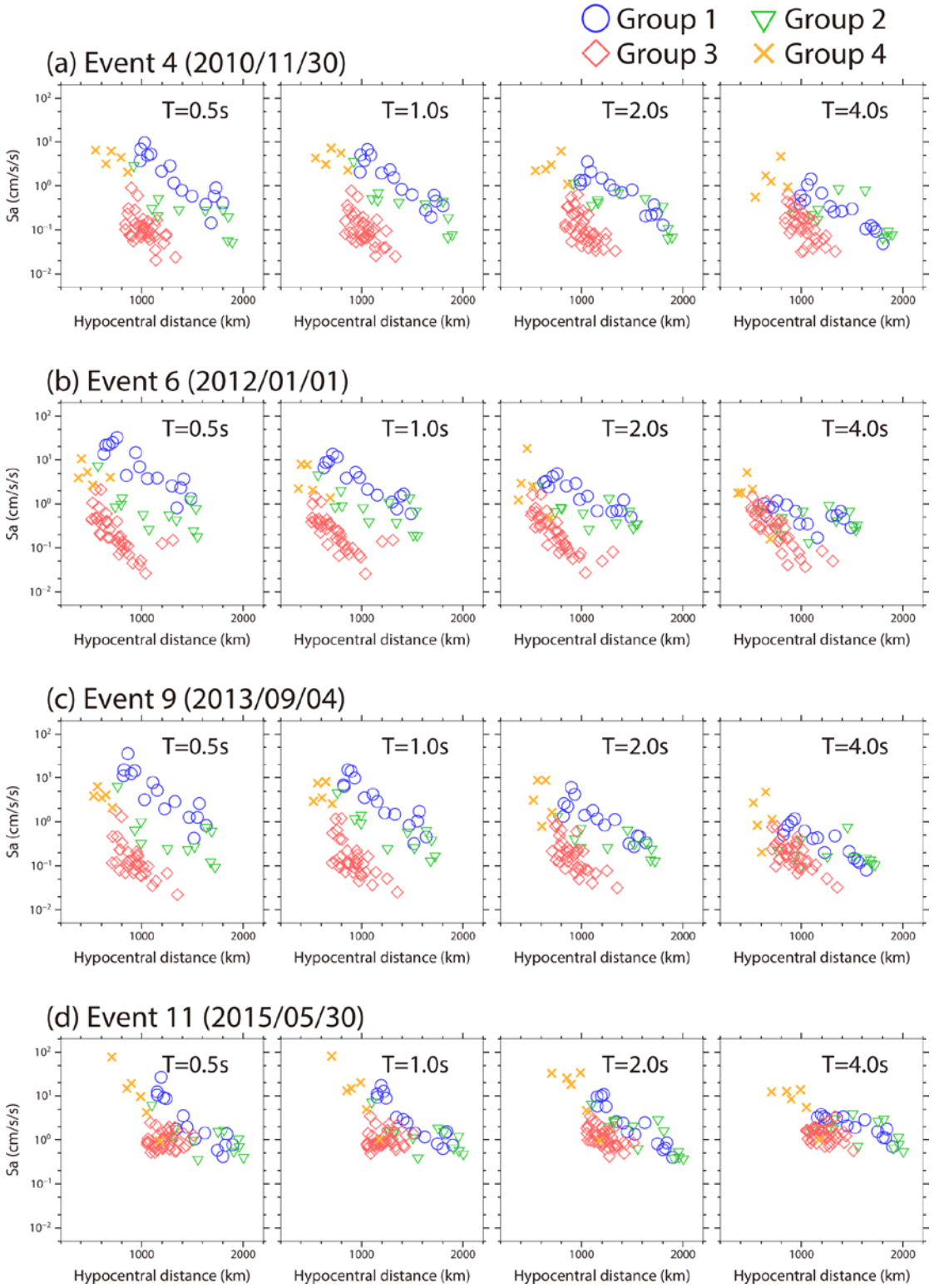

Fig. 4 – Examples of attenuation relationships of 5 % damped acceleration response spectra at 0.5, 1.0. 2.0, and 4.0 s for deep-focus earthquakes around the Ogasawara Islands.

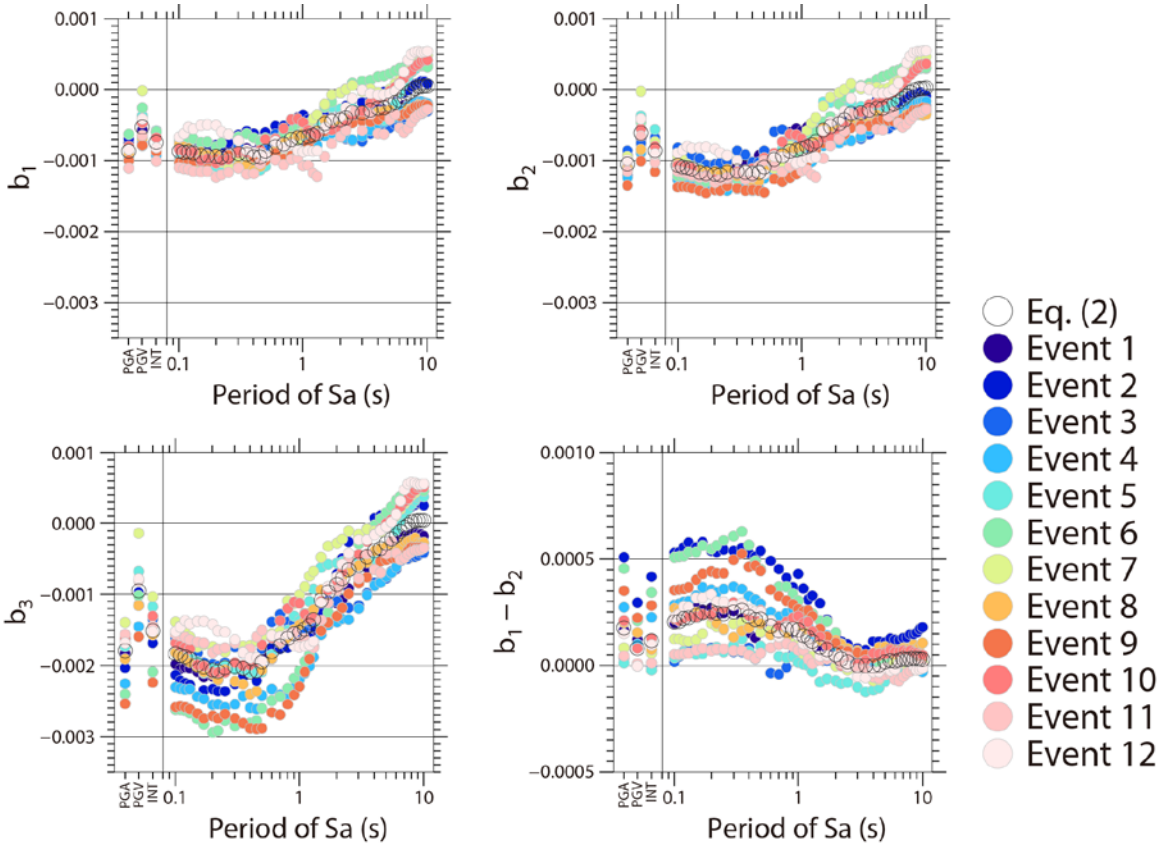

Fig. 5 – Estimated coefficients b_1, b_2, b_3, and b_1-b_2 of Eq. (1) estimated separately for each event

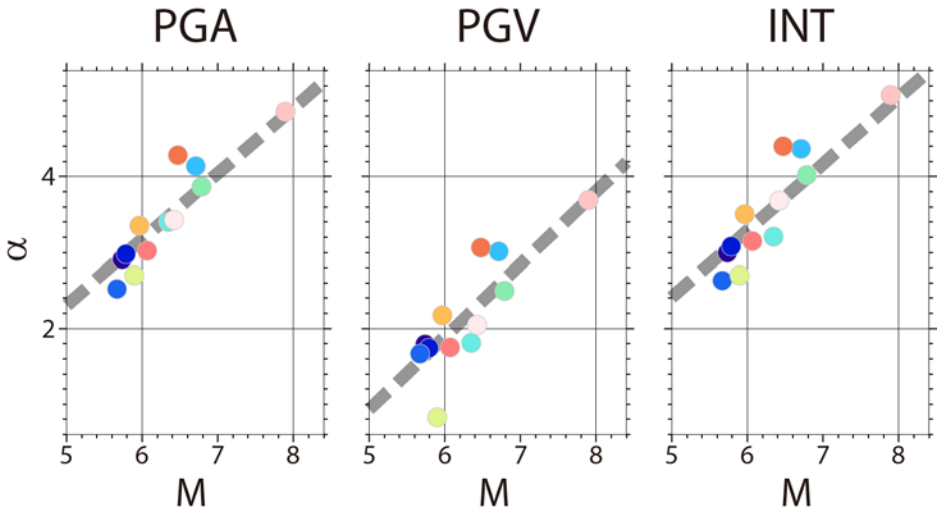

Fig. 6 – Estimated coefficients α of Eq. (1) estimated separately for each event (circles) and M_w -α relationship from estimated coefficients (a, c) of Eq. (2) (broken line)

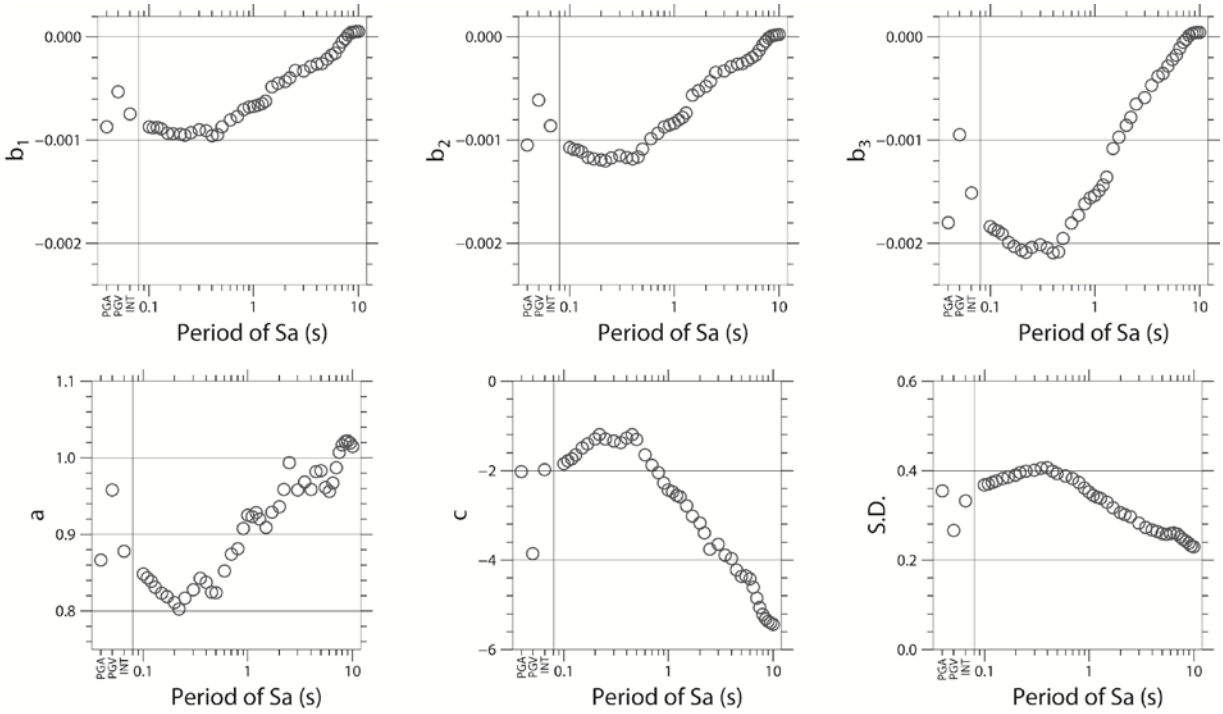

Fig. 7 – Estimated coefficients of Eq. (2) and standard deviation

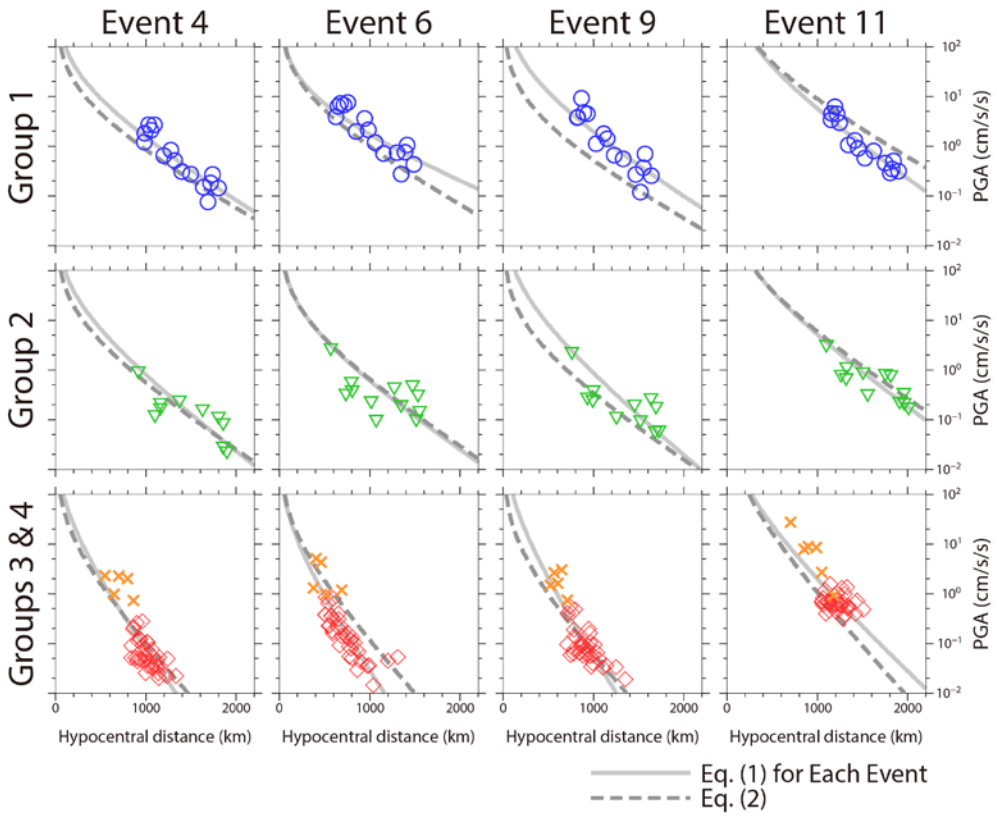

Fig. 8 – Comparison of F-net PGV observations with predicted attenuation relationships from Eq. (1) for each event (solid line) and Eq. (2) (broken line)

Table 1 – List of deep-focus earthquakes around the Ogasawara Islands used in this study

No	Occurrence Time (UTC)	*M*	Depth (km)	Number of F-net station
1	Apr. 19, 2005, 01:46 a.m.	5.7	420	70
2	Mar. 28, 2006, 03:32 p.m.	5.8	440	68
3	Jul. 20, 2008, 09:32 p.m.	5.7	480	63
4	Nov. 30, 2010, 03:24 a.m.	6.7	460	70
5	Jan. 12, 2011, 09:32 p.m.	6.4	600	68
6	Jan. 01, 2012, 05:27 a.m.	6.8	340	71
7	May 26, 2012 09:48 p.m.	5.9	500	67
8	Apr. 21, 2013, 03:22 a.m.	6.0	400	67
9	Sep. 04, 2013, 00:18 a.m.	6.5	440	68
10	Jun. 30, 2013, 07:55 p.m.	6.1	520	70
11	May 30, 2015, 11:23 a.m.	7.9	680	74
12	Jun. 23, 2015, 00:18 p.m.	6.4	480	70